# Fast Sound in Expanded Fluid Hg Accompanying the Metal-Nonmetal Transition

D. Ishikawa,[1,2] M. Inui,[3] K. Matsuda,[1] K. Tamura,[1] S. Tsutsui,[4] and A. Q. R. Baron[4]

[1]*Graduate School of Engineering, Kyoto University, Kyoto, 606-8501, Japan*
[2]*SPring-8/RIKEN 1-1-1 Kouto, Mikazuki-cho, Sayo-gun, Hyogo-ken, 679-5148, Japan*
[3]*Faculty of Integrated Arts and Sciences, Hiroshima University, Higashi-Hiroshima 739-8521, Japan*
[4]*SPring-8/JASRI 1-1-1 Kouto, Mikazuki-cho, Sayo-gun, Hyogo-ken, 679-5198, Japan*

(Received 29 February 2004; published 23 August 2004)

The dynamic structure factor $S(Q, \omega)$ of expanded fluid Hg has been measured up to the metal-nonmetal transition region at 9.0 g cm$^{-3}$ (1723 K and 1940 bars) using high-resolution inelastic x-ray scattering, at momentum transfers, $Q$, from 0.2 to 4.8 Å$^{-1}$. Analysis in the framework of generalized hydrodynamics reveals that the frequencies of the collective excitations increase faster with $Q$ than estimated from the macroscopic speed of sound. The effective sound velocity at 9.0 g cm$^{-3}$ estimated from the dispersion relation is triple the ultrasonic sound velocity. The present result suggests the existence of fast sound in expanded fluid Hg accompanying the metal-nonmetal transition.

DOI: 10.1103/PhysRevLett.93.097801 PACS numbers: 61.25.Mv, 61.10.–i, 71.30.+h

The study of the dynamical properties of fluids is of great importance both in statistical physics and material science. In the last decade, the use of inelastic x-ray scattering (IXS) at third generation synchrotron radiation sources has allowed many new studies of the dynamics of disordered materials. Fast sound in water is a remarkable example among them. An early computer simulation of molecular dynamics [1] predicted high-frequency sound waves almost twice as fast as ordinary sound. Neutron scattering experiments for liquid $D_2O$ was carried out in 1978 [2] and a branch corresponding to the fast sound was first observed in a limited $Q$ range by the second experiment in 1985 [3]. After many studies on fast sound, including computer simulations, IXS experiments for water confirmed the existence of fast-sound waves in a wide $Q$ region approximately twice the low frequency sound velocity [4]. The microscopic origin of the fast-sound effect in liquid water may be explained as an extreme case of positive dispersion, where the average O-O intermolecular distance lies in the repulsive region of an intermolecular pair potential due to a large intermolecular interaction in water [5,6]. We have now observed the excitation energy of the collective mode in expanded fluid Hg near the metal-nonmetal (M-NM) transition to be much higher than expected from low frequency measurements. The effective velocity deduced from the dispersion relation is 1500 m s$^{-1}$ while the ultrasonic sound velocity is 490 m s$^{-1}$ [7,8]. The present observation suggests the existence of fast sound in expanded fluid Hg accompanying the M-NM transition.

Properties of expanded liquid metals have been extensively investigated by heating them along the saturated vapor pressure curve. Liquid Hg, a prototypical liquid metal, undergoes the M-NM transition with volume expansion from 13.6 g cm$^{-3}$ at the ambient condition up to 9 g cm$^{-3}$ near the critical point (critical data of Hg [9]: $T_C = 1751$ K, $P_C = 1673$ bars, and $\rho_C = 5.8$ g cm$^{-3}$). Studies on expanded fluid metals including fluid Hg were reviewed by Hensel and Warren [10]. To clarify the mechanism of the M-NM transition in fluid Hg, it is important to study the structural properties for the expanded fluid. Tamura and Hosokawa [11] carried out x-ray diffraction measurements for expanded fluid Hg. An *ab initio* molecular dynamic simulation by Kresse and Hafner [12] succeeded in explaining the transition at 9 g cm$^{-3}$ in expanded fluid Hg and provided a local structure consistent with that experimentally observed [11]. Recently improved x-ray diffraction data using synchrotron radiation were reported for expanded fluid Hg from liquid to dense vapor [13].

While it is essential to understand the dynamics of fluids, there are few studies on dynamical properties for expanded fluid Hg. Munejiri *et al.* [14] deduced an effective pair potential using experimental data [11] and obtained a dynamic structure factor of expanded fluid Hg by means of a large-scale molecular dynamics simulation. Anomalous sound absorption was reported in expanded fluid Hg at the M-NM transition [15]. These investigations prompted us to measure the dynamic structure factor, $S(Q, \omega)$, of expanded fluid Hg. In this Letter, we report $S(Q, \omega)$ of fluid Hg at densities from 13.6 to 9.0 g cm$^{-3}$, up to the M-NM transition region, obtained using IXS.

This work has been done at the high-resolution IXS beam line (BL35XU) of SPring-8 in Japan [16]. Backscattering at the Si (11 11 11) reflection was used to provide a beam of $3 \times 10^9$ photons/sec in a 0.8 meV bandwidth onto the sample. The energy of the incident beam and the Bragg angle of the backscattering were 21.747 keV and 89.98°, respectively. We used three spherical analyzer crystals at the end of the 10 m horizontal arm to analyze the scattered x rays. The spectrometer resolution was 1.6–1.8 meV (slightly degraded because our large high-pressure vessel forced the detectors about 240 mm

  

away from the sample position) and the momentum transfer resolution was $\Delta Q \sim 0.1$ Å$^{-1}$.

The Hg sample of 99.999% purity and 24 $\mu$m thickness was mounted in a single-crystal sapphire cell [11], and He gas of 99.9999% purity was used as a pressurizing medium. The high-pressure vessel, which can be operated up to 2000 K and 2000 bars, had three Be windows of 10 mm diameter and 10 mm thickness and several smaller windows of 4 mm diameter and 5 mm thickness, so the x rays traveled through 15 mm of Be, 150 mm of He (at high pressure), and the 24 $\mu$m sample. The windows were centered at scattering angles of $2\theta = 1°$, 5°, 10°, 15°, 19°, and 24°, or from 0.2 to 4.83 Å$^{-1}$, and the 10 mm diameter windows permitted the simultaneous use of three analyzer crystals. For the crucial low $Q$ region near the M-NM transition at $\rho = 9$ g cm$^{-3}$, we collected several data sets at different vessel rotations relative to the very small (0.1 mm in diameter) incident beam. This allowed access to a small range of momentum transfers near to 0.2 Å$^{-1}$. We measured IXS spectra for expanded fluid Hg at thermodynamic states [$T$ (K), $p$ (bars), $\rho$ (g cm$^{-3}$)] of (298, 2, 13.6), (773, 50, 12.4), (1273, 500, 11.0), and (1723, 1940, 9.0), and those at $2\theta$ of 1° at several densities from 9 to 4 g cm$^{-3}$. The He gas contributed significant background, especially at low $Q$. The backgrounds were measured at each pressure and temperature and were subtracted after being scaled for sample transmission. The signal from fluid Hg became so large at low $Q$ with volume expansion that we have succeeded in obtaining good quality data.

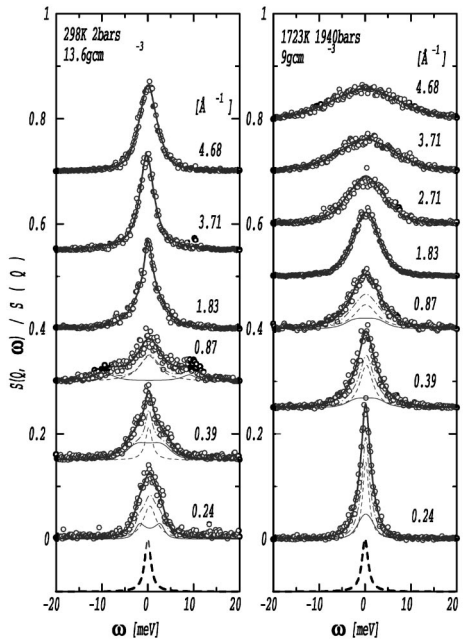


FIG. 1. IXS spectra (open circles) of liquid Hg at densities of 13.6 and 9.0 g cm$^{-3}$ after background subtraction. The experimental data are normalized to their integrated intensity. Fits (solid lines) were made by convoluting the resolution function (dashed line) to a model function (see the text). Also shown are model function (dash-dotted curves), Lorentzian (thin broken curves), and damped harmonic oscillator (DHO) (thin solid curves) terms in the model function at $Q \leq 0.87$ Å$^{-1}$.

Selected IXS data at 13.6 and 9.0 g cm$^{-3}$ are shown in Fig. 1. The integral, $S(Q)$, of the spectrum, $S(Q, \omega)$, was used for the normalization, and $S(Q, \omega)/S(Q)$ are plotted in the figure. The resolution function obtained from a measurement of a polymethyl methacrylate is shown by a broken curve at the bottom. The spectra at 13.6 g cm$^{-3}$ have a clear side peak at around 10 meV at momentum transfer of 0.87 Å$^{-1}$. The spectra agree well with those reported by Hosokawa *et al.* [17]. The IXS spectra at 9.0 g cm$^{-3}$ have a single peak and the side peaks are not distinct from the central one. Note that the central peaks at 3.71 and 4.68 Å$^{-1}$ are much broader at the M-NM transition at 9.0 g cm$^{-3}$ than at ambient conditions, 13.6 g cm$^{-3}$.

We analyzed the data in the framework of generalized hydrodynamics [18]. The spectra were modeled as the sum of Lorentzian at zero energy transfer, representing the thermal contribution, and a DHO [19] for the sound mode with the statistical occupation factor according to Eq. (1). This model has been used with great success in many experiments of liquids and was used previously for the analysis of liquid Hg [17,20]. We take

$$S(Q, \omega)/S(Q) = B(\omega)\left[\frac{A_0}{\pi\Gamma_0}\frac{\Gamma_0^2}{\omega^2 + \Gamma_0^2} + \frac{A_Q}{\pi\beta\hbar} \times \frac{4\omega_Q\Gamma_Q}{(\omega^2 - \Omega_Q^2)^2 + 4\omega^2\Gamma_Q^2}\right], \quad (1)$$

where $B(\omega) = \beta\hbar\omega/[1 - \exp(-\beta\hbar\omega)]$, $\beta = (k_B T)^{-1}$ and $\omega_Q = \sqrt{\Omega_Q^2 - \Gamma_Q^2}$. The parameters $A_0$ and $\Gamma_0$ are the magnitude and the width of a quasielastic peak, while $A_Q$, $\Omega_Q$, and $\Gamma_Q$ are the magnitude, energy, and width of the inelastic excitation. We optimized these parameters by convolving the model function with the measured resolution function and fitting to the data, as shown in Fig. 1. Peaks in the DHO term are well separated at 13.6 g cm$^{-3}$. On the other hand, the DHO term at 9.0 g cm$^{-3}$ has a heavily damped profile even at low $Q$. This behavior suggests a much shorter lifetime of phonons at the M-NM transition and may be related to the observed large ultrasonic sound absorption [15].

Figure 2 shows the $Q$ dependence of the optimized $\Omega_Q$ (squares) at 13.6 and 9.0 g cm$^{-3}$ together with sound velocity (dash-dotted lines) obtained by the ultrasonic measurements [7,8]. Also shown are the normalized second frequency moment $\omega_s(Q)$ (broken curves) and dotted lines with a slope of 1700 m s$^{-1}$ at 13.6 g cm$^{-3}$ and 1500 m s$^{-1}$ at 9.0 g cm$^{-3}$, respectively. Here the second frequency moment is given by

$$\omega_s^2(Q) = \gamma k_B T Q^2/mS(Q), \quad (2)$$

where $m$ and $\gamma$ are the mass of a Hg atom and the specific heat ratio ($C_p/C_V$), respectively. We assumed no $Q$ de-

pendence of $\gamma$ and searched a proper value as a free fit parameter. By taking $\gamma = 1.1$ at 13.6 g cm$^{-3}$ and $\gamma = 1.6$ at 9.0 g cm$^{-3}$, the curves of $\omega_s(Q)$ agree reasonably with the optimized $\Omega_Q$ up to 4.0 Å$^{-1}$, and they seem to be extrapolated towards the dotted lines at low $Q$ where reliable $S(Q)$ was not experimentally obtained.

As seen in Fig. 2, at 13.6 g cm$^{-3}$ $\Omega_Q$ at low $Q$ disperses faster than expected from the sound velocity and agrees with the dotted line of 1700 m s$^{-1}$. The amount of deviation is about 17%, in good agreement with previous work [17]. At 9.0 g cm$^{-3}$, the positive deviation is much more pronounced and the effective velocity, $v_s(Q) = \Omega_Q/Q$, is estimated to be $1500 \pm 200$ m s$^{-1}$, which is triple the ultrasonic sound velocity [7,8]. In the curve fitting with the DHO model shown in Fig. 1, the $\chi^2$ per degrees of freedom for fast sound took values from 1.1 to 1.2 at $Q$ from 0.35 to 0.43 Å$^{-1}$, while that at $Q$ lower than 0.28 Å$^{-1}$ had slightly worse values. Attempts to fit the data from 0.2 to 0.43 Å$^{-1}$ with the ultrasonic velocity lead to unsuitable increases in the $\chi^2$ by a factor of 1.4 on average. The peak position in the current-current correlation function deduced from the optimized model function also indicates that the effective velocity is about 3 times the ultrasonic value. We plot the effective velocity estimated at 0.2–0.43 Å$^{-1}$ as a function of $\rho$ in Fig. 3 together with the sound velocity measured by ultrasonic spectroscopy [7]. The effective velocity of dense Hg vapor from 1.0 to 3.0 g cm$^{-3}$ is taken from a previous paper [21]. In the metallic region, the positive deviation becomes large with volume expansion and has a strong maximum at the M-NM transition. With further volume expansion to the insulating state, the deviation becomes small. Thus, the large positive dispersion, or fast sound, is observed only in a close vicinity of the M-NM transition.

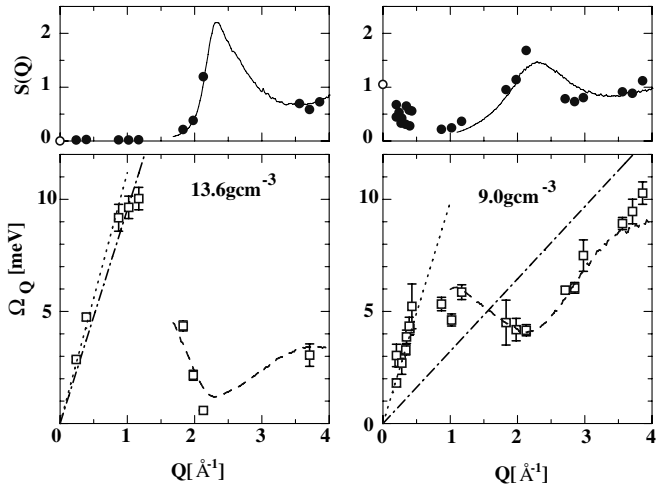


FIG. 2. Excitation energy, $\Omega_Q$ (squares) as a function of $Q$ at densities of 13.6 and 9.0 g cm$^{-3}$. Dash-dotted lines correspond to ultrasonic sound velocity [7,8]. Also shown are the normalized second frequency moment, $\omega_s$ (broken curves), and dotted lines with a slope of 1700 m s$^{-1}$ at 13.6 g cm$^{-3}$ and 1500 m s$^{-1}$ at 9.0 g cm$^{-3}$, respectively. The static structure factor, $S(Q)$ [13] (thin solid curves), the integrated intensity of $S(Q, \omega)$ (closed circles), normalized by the square of the atomic form factor and polarization factor, and $S(0)$ (open circles) calculated from PVT data are indicated in the top figures.

We consider the microscopic dynamics at the M-NM transition. X-ray diffraction experiments suggest that the average number of nearest neighbors within the first coordination shell around an atom is reduced with volume expansion, while the nearest neighbor distance remains unchanged [11,13]. When the coordination number decreases, a change of a single particle motion is expected. In ambient conditions, the line shape of $S(Q, \omega)$ at high $Q$ is similar to a Lorentzian function, which suggests that diffusive motion is dominant in the liquid. With decreasing density, the line shape at high $Q$ broadens, as seen in Fig. 1. To investigate this effect, we carried out fits in the high $Q$ region (4.68 Å$^{-1}$) using a pseudo-Voigt function, which is a weighted combination of Lorentzian and Gaussian curves [22]. The optimized Gaussian fraction $c_G$ at 4.68 Å$^{-1}$ was about 0.5 at ambient conditions. However, the $c_G$ became 0.8 at the M-NM transition at 9.0 g cm$^{-3}$. This suggests that at 9.0 g cm$^{-3}$ a free particle motion is dominant over short (less than interatomic) distances. We note that the value of $\gamma$ of 1.6 estimated from the present data seems consistent with this result, being close to the value of a monatomic ideal gas, $\gamma = 5/3$.

We discuss the fast sound observed at the M-NM transition. The adiabatic compressibility, $\chi_s$, is calculated from sound velocity by $\chi_s = (\rho v_s^2)^{-1}$. The fast-sound velocity suggests that the microscopic $\chi_s$ is much smaller than the macroscopic one, which means that the mean square fluctuations of microscopic pressure, $\langle(\Delta p)^2\rangle \propto \chi_s^{-1}$, are very large. The enhancement of microscopic $\langle(\Delta p)^2\rangle$ can be caused by a local deformation of a pair potential, $\phi(r)$, especially its repulsive part, as shown by the pressure equation,

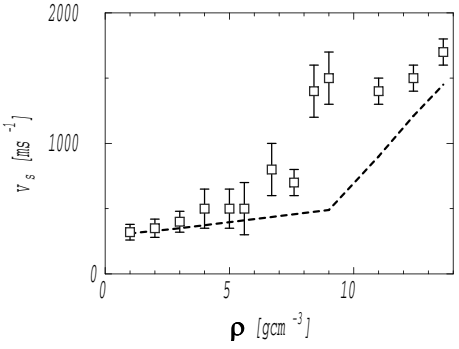


FIG. 3. Density dependence of sound velocity taken from the data at low $Q$ (0.2–0.43 Å$^{-1}$). The dashed line is the ultrasonic sound velocity from [7], while the three lowest points (1–3 g cm$^{-3}$) are from [21]. See the text for discussion.

$$p = nk_BT - (n^2/6)\int r(\partial\phi/\partial r)g(r)d\mathbf{r}, \qquad (3)$$

where $n$ is a number density and $g(r)$ is a pair distribution function. We expect such a deformation in a pair potential being pronounced at the M-NM transition, due to the large fluctuations of local electronic states between metallic and insulating ones. A sign of fluctuations at the M-NM transition may be found in the present data such as the narrowing of $S(Q, \omega)$ at 0.24 $\text{Å}^{-1}$ at 9.0 $\text{g cm}^{-3}$ compared with at ambient conditions, and the rapid increase of $S(Q)$ at low $Q$ with $Q \to 0$. Thus the appearance of the fast sound strongly hints that the M-NM transition accompanies intrinsic fluctuations induced by the local deformation of a pair potential. We speculate that pressure fluctuations in microscopic space and time where the fast-sound waves exist are averaged and smoothed out as the thermodynamic limit is approached.

Finally we comment on the discrepancy between our microscopic $\gamma$ estimated from the measured dispersion and Eq. (2), and the macroscopic thermodynamic value. Levin and Schmutzler [23] measured $C_p$ for expanded fluid Hg from 12.4 to 8.8 $\text{g cm}^{-3}$ and deduced $C_V$ using PVT data and a thermodynamic relation. The $\gamma$ calculated from their data is 1.2 at 12.4 $\text{g cm}^{-3}$ and 3.6 at 9.0 $\text{g cm}^{-3}$. Alternatively, using sound velocity, PVT data, and the relation, $\gamma = \chi_T/\chi_s$, where $\chi_T$ is the isothermal compressibility, results similar to those by Levin and Schmutzler were reported [24,25]. While our value of $\gamma$ agrees with the thermodynamically determined ones near ambient conditions, we see a much smaller value at low densities near the M-NM transition. We speculate that this results from the microscopic character of the IXS measurements, which probe both small volumes and high frequencies, and represents the essence of the M-NM transition. Microscopically observed $\chi_s$ is small, so the fact that $\gamma$ is small means $\chi_T$ must be small, which means that the microscopic mean square fluctuations of a particle number, $\langle(\Delta N)^2\rangle \propto \chi_T$, are small. In contrast, the thermodynamic measurements appear providing the results commonly observed that for low densities approaching the critical point $\gamma$ diverges as the macroscopic $\langle(\Delta N)^2\rangle$ becomes large. The characteristic nature of the fluctuation in the M-NM transition is that the microscopic $\langle(\Delta p)^2\rangle$ is large and $\langle(\Delta N)^2\rangle$ is small.

In summary, we have measured the dynamic structure factor of expanded fluid Hg up to the M-NM transition region. While damping of the collective mode increases with volume expansion, we obtained an effective sound velocity that is much faster than the low frequency sound velocity at the M-NM transition. The appearance of fast sound may represent fluctuations intrinsic to the M-NM transition. Additional IXS experiments for expanded fluid Hg are under way to obtain the $\omega$-$Q$ dispersion relation in a wider density range. It may be effective to observe a long range structure in expanded fluid Hg at the M-NM transition by means of small angle x-ray scattering.

The authors thank Professor K. Hoshino, Professor F. Shimojo, and Mr. S. Tanaka for their valuable discussions, and Dr. T. Ishikawa and Dr. Y. Tanaka for their support of this project. The authors acknowledge Mr. H. Itoh, Mr. Y. Itoh, Mr. K. Satoh, Mr. K. Mifune, Ms. M. Kusakari, Mr. Y. Naitoh, and Mr. M. Muranaka for their support of the present experiment. Kobe Steel Co. Ltd. and High-Pressure System Co. Ltd. are acknowledged for their technical support. This work is supported by the Grant-in-Aid for Specially Promoted Research from the Ministry of Education, Science and Culture of Japan under Contract No. 11102004. The synchrotron radiation experiments were performed at the SPring-8 with the approval of the Japan Synchrotron Radiation Research Institute (JASRI) (Proposals No. 2003A6607-LD-np and No. 2003B0206-ND3d-np).

[1] A. Rahman and F. H. Stillinger, Phys. Rev. A **10**, 368 (1974).
[2] P. Bosi *et al.*, Nuovo Cimento Lett. **21**, 436 (1978).
[3] J. Teixeira *et al.*, Phys. Rev. Lett. **54**, 2681 (1985).
[4] F. Sette *et al.*, Phys. Rev. Lett. **75**, 850 (1995).
[5] U. Balucani *et al.*, Phys. Rev. E **47**, 1677 (1993).
[6] G. Ruocco and F. Sette, J. Phys. Condens. Matter **11**, R259 (1999).
[7] M. Yao *et al.*, J. Non-Cryst. Solids **205–207**, 274 (1996).
[8] V. Kozhevnikov *et al.*, J. Non-Cryst. Solids **205–207**, 256 (1996).
[9] W. Gözlaff *et al.*, Z. Phys. Chem. Neue Folge **156**, 219 (1988).
[10] F. Hensel and W. W. Warren, Jr., *Fluid Metals* (Princeton University Press, Princeton, NJ, 1999).
[11] K. Tamura and S. Hosokawa, Phys. Rev. B **58**, 9030 (1998).
[12] G. Kresse and J. Hafner, Phys. Rev. B **55**, 7539 (1997).
[13] M. Inui *et al.*, Phys. Rev. B **68**, 094108 (2003).
[14] S. Munejiri *et al.*, J. Phys. Condens. Matter **10**, 4963 (1998).
[15] H. Kohno and M. Yao, J. Phys. Condens. Matter **13**, 10 293 (2001).
[16] A. Baron *et al.*, Nucl. Instrum. Methods Phys. Res., Sect. A **467–468**, 627 (2001).
[17] S. Hosokawa *et al.*, J. Non-Cryst. Solids **312–314**, 163 (2002).
[18] J. P. Boon and S. Yip, *Molecular Hydrodynamics* (McGraw-Hill, New York, 1980).
[19] B. Fåk and B. Dorner, Institute Laue-Langevin Report No. 92FA008S, 1992.
[20] L. E. Bove *et al.*, Phys. Rev. Lett. **87**, 215504 (2001).
[21] D. Ishikawa *et al.*, J. Phys. Condens. Matter **16**, L45 (2004).
[22] P. Thompson *et al.*, J. Appl. Crystallogr. **20**, 79 (1987).
[23] M. Levin and R. Schmutzler, J. Non-Cryst. Solids **61 & 62**, 83 (1984).
[24] K. Suzuki *et al.*, J. Phys. (Paris), Colloq. **41**, C8-66 (1980).
[25] M. Yao and H. Endo, J. Phys. Soc. Jpn. **51**, 966 (1982).